Water Research 290 (2026) 125127

Contents lists available at ScienceDirect

Water Research

journal homepage: www.elsevier.com/locate/watres

Coupled nitrogen–pollutant photochemistry: Marine nitration of ethylparaben and formation of toxic nitro-products

Yanpeng Gao [a,b], Yi Chen [a,b], Suling Wei [a,b], Yashi Bi [a,b], Yujie Chen [a,b], Guanhui Chen [a,b], Xiaolin Niu [a,b], Na Luo [a,b], Yuemeng Ji [a,b], Yang-Guang Gu [c,*]

[a] Guangdong-Hong Kong-Macao Joint Laboratory for Contaminants Exposure and Health, Guangdong Key Laboratory of Environmental Catalysis and Health Risk Control, Institute of Environmental Health and Pollution control, Guangdong University of Technology, Guangzhou 510006, China
[b] Guangdong Basic Research Center of Excellence for Ecological Security and Green Development, Key Laboratory of City Cluster Environmental Safety and Green development of the Ministry of Education, School of Environmental Science and Engineering, Guangdong University of Technology, Guangzhou 510006, China
[c] South China Sea Fisheries Research Institute, Chinese Academy of Fishery Sciences, Guangzhou 510300, China

HIGHLIGHTS

- Marine environments markedly enhance the photochemical degradation of ethylparaben compared with ultrapure and estuarine waters.
- Reactive nitrogen species drive the marine nitration of ethylparaben, yielding nitro-products absent in ultrapure water systems.
- The nitration follows a light-induced coupling pathway between reactive nitrogen species and organic pollutants in seawater.
- The nitro-derivative exhibits stronger ERα binding affinity and higher endocrine-disrupting potency than the parent compound.
- This work identifies a novel nitrogen–pollutant photochemical coupling mechanism posing emerging risks to coastal ecosystems.

GRAPHICAL ABSTRACT

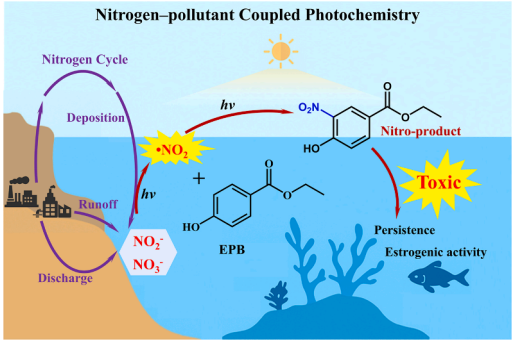

ARTICLE INFO

Keywords:
Reactive nitrogen species (RNS)
Marine photochemistry
Ethylparaben
Nitration mechanism
Toxic nitro-products
Pearl River Estuary

ABSTRACT

Nitrogen enrichment and emerging pollutants frequently co-occur in marine environments, yet their coupled photochemical behavior remains poorly understood. This study reveals that coastal seawater significantly enhances the sunlight-driven transformation of ethylparaben (EPB), a typical preservative, compared with ultrapure and estuarine waters. Remarkably, nitration of EPB occurs in seawater and estuarine water, yielding nitro-products ethyl 4-hydroxy-3-nitrobenzoate (NO_2-EPB) that are absent in ultrapure water. Mechanistic investigations indicate that photo-induced reactive nitrogen species (RNS), particularly nitrogen dioxide radical ($\bullet NO_2$) derived from nitrate and nitrite photolysis, are key drivers of this transformation of EPB. The resulting nitro-products display greater persistence and substantially higher predicted toxicity toward marine organisms than the parent compound. These findings uncover a previously unrecognized nitrogen–pollutant coupled

* Corresponding author. South China Sea Fisheries Research Institute, Chinese Academy of Fishery Sciences, Guangzhou 510300, China.
E-mail address: sunshinegu@scsfri.ac.cn (Y.-G. Gu).

https://doi.org/10.1016/j.watres.2025.125127
Received 19 October 2025; Received in revised form 23 November 2025; Accepted 8 December 2025
Available online 9 December 2025

photochemistry in coastal ecosystems, illustrating how anthropogenic nitrogen loading can alter the environmental fate and risks of emerging contaminants. This work provides new insight into the synergistic roles of reactive nitrogen and solar irradiation in shaping contaminant behavior in marine waters, emphasizing the overlooked pathways that may amplify ecological hazards in nitrogen-rich coastal zones.

1. Introduction

Nitrogen loading to marine environments has substantially increased over the past decades due to intensive agricultural activities, wastewater discharge, and atmospheric deposition (Gong et al., 2024). Large quantities of nitrate (NO_3^-) and nitrite (NO_2^-) are continuously delivered to coastal waters worldwide, profoundly altering marine biogeochemical cycles and photochemical processes (Godfrey et al., 2025; Liu et al., 2025). At the same time, the widespread use of personal care products has led to the continuous input of emerging pollutants such as parabens—alkyl esters of p-hydroxybenzoic acid—into aquatic systems (Bolujoko et al., 2022; Lu et al., 2023; Wei et al., 2021; Zhu et al., 2024). Particularly, ethylparaben (EPB) is frequently detected in coastal seawater at concentrations ranging from nanograms to micrograms per liter (Peng et al., 2025; Xue et al., 2017), raising concerns about its persistence and potential endocrine-disrupting effects.

Despite the extensive attention given to nutrient pollution and organic micropollutants (Baker et al., 2021; Du et al., 2025; McDowell et al., 2025; Schwarzenbach et al., 2006; Tait et al., 2023; Wang et al., 2024, 2023; Wilkinson et al., 2022), previous studies have mostly evaluated their environmental behaviors independently. For nutrient pollution, numerous studies have characterized the photochemical behaviors of NO_3^- and NO_2^-, including the generation of reactive intermediates such as hydroxyl radical (•OH), nitrogen dioxide radical ($•NO_2$) and peroxynitrite, and their roles in oxidative processes in natural waters (Benedict et al. 2017; Chen et al. 2019, Vione et al., 2005). Notably, nitration and nitrosation intermediates are primarily formed via reactive nitrogen species (e.g. $•NO_2$ and peroxynitrite) generated via NO_3^- and NO_2^- photolysis (Yin et al. 2024), whereas •OH plays a minor role. In parallel, studies on organic micropollutants have increasingly elucidated their direct and indirect photo-transformation pathways, photoproducts formation under environmentally relevant conditions, and associated toxicity evolution (Fang et al. 2013; Gao et al. 2014; Niu et al. 2025). Nevertheless, little is known about their coupled photochemical interactions in sunlit marine waters, particularly the role of reactive nitrogen species in driving the transformation and nitration of emerging contaminants such as EPB. In sunlit surface waters, nitrogen species such as NO_3^- and NO_2^- can undergo photolysis to generate reactive intermediates (e.g., •OH, $•NO_2$, and peroxynitrite), which are capable of reacting with coexisting organic contaminants (Bu et al., 2020; Ge et al., 2019; Marussi and Vione., 2021; Scholes et al., 2019; Scholes., 2022; Vione., 2022). Such interactions may lead to the formation of unexpected and potentially more toxic transformation products (Gong et al., 2022; Wu et al., 2020). The coupled nitrogen–pollutant photochemistry thus represents an important yet understudied process governing contaminant fate in marine ecosystems.

Recent research has begun to recognize that nitrate- or nitrite-mediated photo-transformations can modify the degradation pathways of aromatic compounds (Palma et al., 2020; Zhou et al., 2020). Nevertheless, most of these studies were performed in freshwater or ultrapure water systems (Vione, 2022; Zhang et al., 2022), neglecting the complex ionic composition and light field characteristics of marine environments. The presence of high salinity and dissolved organic matter (DOM) in seawater can strongly influence photochemical reaction pathways (Calza et al. 2012; Wang et al., 2020), potentially favoring nitration of organic substrates. For example, halides and carbonate species in seawater modulate the steady-state levels of $•NO_2$ and substrate-derived radicals, suppressing halogenation and promoting selective formation of nitro-products, while DOM can both screen light and sensitize radical formation, further facilitating nitration (Calza et al. 2012). These characteristics make marine environments particularly suitable for investigating nitrogen–pollutant coupled photochemistry, as the combined effects of salinity, carbonate species, and DOM create a reactive matrix that is absent in freshwater systems. As a result, marine environments are generally more susceptible to the formation of nitration products than freshwater systems, due to the synergistic effects of salinity and DOM on reactive nitrogen species. Despite this enhanced reactivity, the occurrence and environmental implications of nitrogen–pollutant coupled photochemical transformations in marine systems remain poorly understood.

In this study, we investigated the photochemical transformation of EPB under collected natural seawater containing reactive nitrogen species, aiming to elucidate potential nitrogen–pollutant coupling mechanisms. Concurrently, parallel photolysis experiments of EPB were performed in natural estuarine water and ultrapure water as control matrices. Particular attention was given to the possible marine nitration of EPB and the generation of nitro-products, which have not been reported in ultrapure water systems. To better understand their environmental relevance, we further evaluated the potential estrogenic activity and receptor-binding affinity of the nitration products through theoretical toxicity prediction. This study provides new insights into how nitrogen enrichment and emerging pollutants jointly influence photochemical transformation processes in coastal seawater. It highlights the environmental significance of coupled nitrogen–pollutant photochemistry, whereby nutrient pollution not only drives eutrophication but also facilitates the formation of secondary toxic products through light-induced reactions. Understanding these interactions is essential for assessing the fate and ecological risks of emerging contaminants in nitrogen-rich marine ecosystems.

2. Materials and methods

2.1. Chemicals

EPB (99 % purity) was obtained from Tokyo Chemical Industry, Japan. Ethyl 4-hydroxy-3-nitrobenzoate (NO_2-EPB, 95 % purity) was provided by Yuanye Biotechnology Co., Ltd. (Shanghai, China). The HPLC-grade acetonitrile and methanol were respectively purchased from Sigma-Aldrich (St. Louis, MO, USA) and Macklin Biochemical Co., Ltd. (Shanghai, China). Solid phase extraction (SPE) cartridges (Oasis HLB, 3cc, 60 mg) were purchased from Waters. All laboratory water was prepared with ultrapure water (18.25 MΩ·cm, Millipore Corp, Burlington, MA, USA).

Estuarine water samples were collected from the Pearl River Estuary, Guangdong Province, China. Seawater samples were collected from the coastal waters of the South China Sea, China. All water samples were immediately filtered through glass fiber filters (0.22 μm pore size, Xingya, Shanghai, China) to remove suspended particles and microorganisms after collection. This procedure has been widely used to eliminate potential biodegradation when investigating the abiotic degradation of chemicals (Peng et al., 2022). To minimize potential matrix effects associated with the high ionic strength of seawater during anion analysis, filtered samples were pre-treated prior to measurement and quantified using matrix-matched calibration standards. The collected and processed samples were stored in brown glass bottles and placed in a refrigerator at 4 °C, protected from light. Detailed sampling information and water quality parameters for both estuarine and seawater samples were listed in Table S1.

2.2. Photochemical transformation experiments

Photochemical transformation experiments of EPB were conducted using an MC-PHCAIO multifunctional photochemical reactor (Beijing Merry Change Technology Co., Ltd., China). The reactor was equipped with a quartz cold trap, a circulating cooling water system, and a rotary stirrer system. The reaction temperature was 25±1 °C. The radiation source was a 500 W xenon lamp. Its radiation spectrum was measured (Fig. S1), and this lamp can be used to simulate sunlight irradiation. The xenon lamp was positioned in a cylindrical quartz cold trap at the center of the reactor. The light intensity on the surface of the reaction tube was 45 mW/cm^2, as measured using an optical power meter (PL-MW2000, Beijing Perfectlight, China), which is within the range of sunlight intensity (Troughton et al., 2018).

This study used coastal seawater from the South China Sea as a representative marine matrix, and concurrently conducted comparative photodegradation experiments of EPB in Pearl River Estuary water (estuarine system) and ultrapure water. EPB was dissolved in these matrices at an initial concentration of 1 mg L^{-1}. This elevated concentration was intentionally selected to ensure clear identification of transformation pathways, as environmentally relevant levels of EPB often fall near or below the instrumental detection limit, potentially obscuring low-yield intermediates. To simulate diurnal solar irradiation, the solutions were irradiated under a xenon lamp at 450 W/m^2, corresponding to solar irradiance at a 30° solar elevation on a clear midsummer day, using a 12 h light/ 12 h dark cycle. This light-dark cycle was conducted over a total period of 48 h, simulating two days. We acknowledge that solar irradiance naturally varies throughout the day, peaking at noon when the solar zenith angle is lowest; although lamp intensity could not be dynamically adjusted, this setup closely mimics environmental conditions. Outdoor sunlight experiments were also conducted to confirm that the observed transformations occur under real environmental conditions. During the entire experimental period, aliquots of the reaction solution were collected at specific time. For the actual water samples (seawater and estuarine water), 5 mL of the reaction sample was taken for enrichment and concentration using SPE cartridges (detailed procedures are described in Text S1); for the ultrapure water samples, 1 mL of the reaction sample was collected. All withdrawn reaction samples were subjected to EPB concentration analysis and photochemical degradation product identification. The SPE recovery of the primary photoproduct NO_2-EPB was determined to be 90 %, meeting the accuracy requirements for quantitative analysis, and verified to fall within the acceptable range (see Text S1 in Supplementary Information) Dark control experiments were run in parallel by covering the quartz test tubes with aluminum foil to block all light. All experiments were conducted in triplicate to ensure repeatability.

2.3. Analysis of the concentration of EPB and transformation products

The peak areas of EPB and its transformation products were determined using a high-performance liquid chromatography quadrupole-time of flight tandem mass spectrometry (HPLC-QTOF-MS) instrument (Agilent G6545B, USA). Electrospray ionization (ESI) mass spectrometry (MS) was conducted in the negative ion mode with a fragmentor voltage of 175 V. Argon was used as the collision gas, and different collision energies were applied for daughter ion analysis. Chromatographic separation was performed using a Waters ACQUITY UPLC BEH C18 column (2.1 × 100 mm, 1.7 μm particle size). The mobile phase consisted of a mixture of acetonitrile (solvent A) and ultrapure water containing 0.1 % formic acid (solvent B). The gradient elution program was as follows: 10 % A was used initially and maintained for 3 min; then it was linearly increased to 50 % A over 26 min; finally, the gradient returned to 10 % A and was maintained for another 3 min. The reaction solution samples were directly analyzed at an eluent flow rate of 0.3 mL/min. The data obtained were analyzed using Qualitative Analysis (Agilent Technologies, B.08.00) software and MassHunter Profinder (Agilent Technologies, version 10.0).

2.4. Determination of NO_3^- and NO_2^- concentrations

The determination of NO_3^- involved pre-treatment of the water sample, which was carried out by adding 1 mL of LH—NO_3-BSS1 reagent to 5 mL of the water sample and 1 mL of distilled water (blank) respectively, and then thoroughly shaking. Next, 4 mL of LH—NO_3-BSS2 reagent was placed in a reaction tube, and 1 mL of the blank solution and 1 mL of the pre-treated water sample were added respectively. The cap was tightly closed, and the tube was shaken immediately 10 times. The tube was then placed in a cold water bath for 10 min. Afterward, the solution was poured into a 16 mm cuvette, which was placed in the ultraviolet-visible intelligent multi-parameter water quality analyzer (LH-3BA (V12), Lianhua Technology, China) for blank calibration prior to color reading. The determination of NO_2^- involved adding 0.2 mL of LH—$NO_2$2 reagent to 10 mL of the water sample and distilled water (blank) respectively. The mixture was shaken and allowed to stand for 20 min. The solution was poured into a 3 cm cuvette, which was placed in the instrument for blank calibration before color reading.

2.5. Theoretical calculations

All quantum chemical calculations were performed using Gaussian 09 software (Frisch et al., 2009). The geometric configurations of all reactants, intermediates, transition states, and products were fully optimized at the B3LYP/6–311 g(d,p) level in water using the SMD implicit solvent model (Marenich et al., 2009; Zhao and Truhlar, 2008). Vibrational frequency calculations were conducted at the same level to confirm that each stationary point corresponded to either a minimum (no imaginary frequencies) or a transition state (one imaginary frequency). Intrinsic reaction coordinate (IRC) calculations were further performed to verify that each transition state was correctly connected to the corresponding reactants and products. Single-point energy calculations were subsequently refined at the B3LYP/6–311++G(3df,2p) level.

Molecular docking was performed using the Autodock 4.2.6 software package. The three-dimensional crystal structure of the Pacific oyster estrogen receptor α (ERα) (PDB ID: 4N1Y) was downloaded from the Protein Data Bank (PDB) database (https://www.rcsb.org/structure/4N1Y). PyMOL (Version 2.5.2) was employed to remove water molecules and the original ligand from the protein structure. Subsequently, the AutoDockTools software was used to generate the docking grid box parameter files for the protein and ligand based on the ligand-binding pocket of the ligand-binding domain (LBD), with the grid box dimensions set to 126 Å × 126 Å × 126 Å. The Lamarckian Genetic Algorithm (LGA) was selected as the docking engine, and the number of molecular docking runs was set to 100, while the remaining parameters were kept as default. After completing the docking simulation, the final results were visualized using PyMOL. The half-maximal inhibitory concentration (IC_{50}) represents the concentration of a compound required to inhibit 50 % of the estrogen receptor binding activity, reflecting its binding affinity to the receptor ERα and thus indicating its potential estrogenic activity (Niu et al., 2025). Key environmental fate parameters, including the hydrophobicity, bioconcentration factor (BCF), and organic carbon–water partition coefficient (Koc) of EPB and NO_2-EPB were predicted using the USEPA EPI Suite (USEPA 2012). Mutagenicity and carcinogenicity were further predicted using the Danish (Q)SAR Models platform (MEFD, 2025), which provides a probability value and a qualitative prediction, and applicability domain information. These predictions were used to evaluate the potential toxicological risks and bioaccumulation tendencies of the compounds.

3. Results and discussion

3.1. Photochemical degradation behavior of EPB under marine conditions

To explore the photochemical behavior of EPB in marine environments, simulated diurnal irradiation experiments were conducted using seawater from the South China Sea (Sites S1 and S2 in Fig. 1). The concentration of EPB decreased significantly under light exposure, following first-order kinetics (Fig. S2). After 48 h of irradiation, 68.5 % of EPB at Site S1 and 58.7 % at Site S2 were degraded (Fig. 1), corresponding to overall rate constants of 0.028 h^{-1} and 0.020 h^{-1}, respectively. During the daytime phase, degradation rates were substantially higher (0.04338 h^{-1} for 0–12 h and 0.03046 h^{-1} for 24–36 h at Site S1) than during the nighttime phase (0.00722 h^{-1} for 12–24 h and 0.0002 h^{-1} for 36–48 h), highlighting the dominant role of photochemical processes in EPB transformation relative to non-photochemical processes such as hydrolysis. The faster degradation observed at Site S1 compared to Site S2 underscores the significant impact of local seawater properties on transformation efficiency. Detailed photochemical degradation kinetics are provided in Text S2.

The concentrations of NO_3^- and NO_2^-, key inorganic nitrogen species, were determined to elucidate their effects on EPB degradation. Site S1 exhibited higher NO_3^- (0.332 mg/L) and comparable NO_2^- (0.024 mg/L) than Site S2 (0.066 and 0.026 mg/L, respectively) (Fig. 1d). Given that NO_3^- and NO_2^- can act as photosensitizers and sources of reactive nitrogen species (RNS) and •OH upon light irradiation (Rayaroth et al., 2022; Scholes et al., 2019), the higher NO_3^- level at Site S1 likely enhanced RNS and •OH production, thus accelerating EPB degradation. Moreover, the coexistence of NO_3^- and NO_2^- increases both the diversity and concentration of reactive species (Palma et al. 2020; Vione et al. 2002), leading to a synergistic enhancement of EPB photolysis. In particular, •OH generated from NO_3^- photolysis can oxidize NO_2^- to $•NO_2$, a key nitrating species that drives the formation of nitro-products. (Gong et al., 2022; Li et al., 2021). Consequently, the coupled nitrogen–pollutant photochemistry driven by NO_3^-/NO_2^- cycling is more active at Site S1, promoting both EPB degradation and the formation of nitrated transformation products.

These results indicate that the marine nitrogen environment may influence both EPB degradation kinetics and the potential transformation pathways by generating reactive species. Compared with estuarine and ultrapure water systems (Fig. 2; Text S3), the open marine system could provide a more favorable setting for coupled nitrogen–pollutant photochemistry, potentially due to the coexistence of

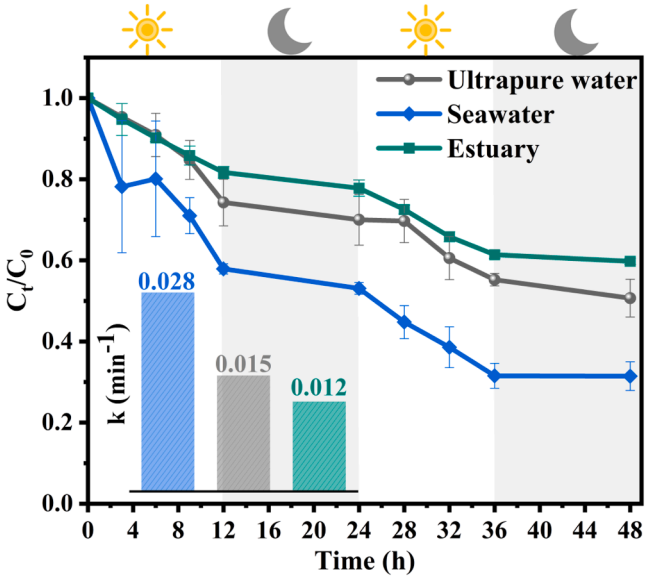

Fig. 2. Photochemical transformation curves of EPB in seawater, estuarine water, and ultrapure water under simulated diurnal solar irradiation. Error bars represent the standard deviation of three independent replicates. The inset shows the degradation rate constants of EPB over 48 h.

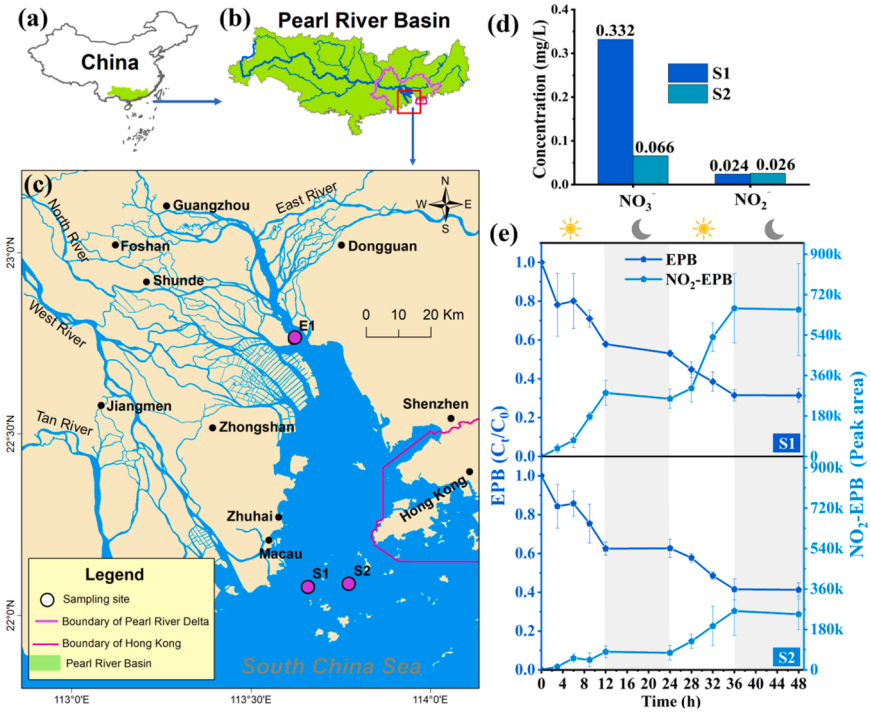

Fig. 1. (a) Map of China; (b) location of the Pearl River Basin on the map of China; (c) the positions of Site S1 and S2 in the Pearl River Basin; (d) comparison of NO_3^- and NO_2^- concentrations at Site S1 and Site S2; (e) photochemical degradation curves of EPB and peak area of the formed NO_2-EPB at Site S1 and Site S2 under simulated diurnal solar irradiation.

abundant DOM, inorganic ions, salinity, and sunlight penetration. Although the exact contribution of each factor remains to be fully elucidated, these observations suggest that the coupling effects may contribute to differences in EPB photochemistry between marine, estuarine, and ultrapure waters, highlighting the potential complexity for reaction dynamics in open marine systems.

3.2. Identification and characterization of nitration-dominated transformation products

The products formed during the photochemical degradation of EPB were separated and identified using HPLC-TOF-MS and MassHunter Profinder. The extracted ion chromatograms (EICs) and fragmentation patterns of the transformation products are provided in Fig. 3 and Fig. S3. Table S2 compiles the [M-H]$^-$ ion (m/z), retention time (RT), mass accuracy (ppm), and structure of each product, along with the confidence level of each product based on the Schymanski scale (Schymanski et al., 2014). The result showed that two major chromatographic peaks corresponding to the parent compound EPB and a nitrated transformation product, identified as nitro-ethylparaben (NO_2-EPB), and further confirmed using the authentic NO_2-EPB standard (Fig. 3). The detailed analysis process procedure is provided in Text S4 of the Supplementary material. Additionally, it is worth noting that no hydroxylated products (OH-EPB), which are commonly observed in ultrapure water system and in previous studies (Gao et al., 2020; Niu et al., 2025), were detected in the marine experiments (Fig. S3). This indicates a distinct transformation pathway in seawater, dominated by nitration rather than hydroxylation.

The absence of OH-EPB during EPB transformation in seawater is most likely due to the high photoreactivity of the hydroxylated products, resulting in their further photodegradation following formation (Ge et al. 2016; Niu et al. 2025). Additionally, major marine constituents such as bicarbonate, carbonate, and natural organic matter can scavenge of •OH, further suppressing the accumulation of hydroxylated products (Bu et al., 2020; Li et al., 2021). Under such conditions, the photochemically generated •NO_2, which originates directly from nitrate photolysis and from the reaction of nitrite with •OH, becomes the predominant reactive species, selectively inducing electrophilic substitution on the phenolic ring of EPB to yield NO_2-EPB. This mechanistic shift exemplifies the coupled nitrogen–pollutant photochemistry, where nitrogen species actively redirect the transformation pathway toward nitration-dominated reactions.

Further kinetic analysis demonstrated that NO_2-EPB formation occurred exclusively under light irradiation and ceased during dark periods (Fig. 4), confirming its photochemical origin. During the first 12 h of light exposure, the formation rate of NO_2-EPB was 0.062 mg L^{-1} h^{-1}, and the yield increased from 0 % to 13.1 %. During the second light cycle, the rate increased to 0.089 mg L^{-1} h^{-1} with the yield reaching 30.6 % (Fig. 4). In contrast, degradation in dark periods was negligible (<3.5 %), suggesting that light is the primary driver of NO_2-EPB formation and that nitration represents an important pathway in EPB photochemical transformation. This observation further indicates that NO_2-EPB is relative stable under the tested dark conditions, although its persistence under natural environmental factors remains to be investigated. In addition, compared to the estuarine system, the open marine system favors coupled nitrogen–pollutant photochemistry, resulting in higher absolute concentrations of nitro-products (Fig. 4). Notably, quantum chemical calculations supported an electrophilic substitution nitration mechanism as the most favorable pathway, involving an exothermic direct attack of •NO_2 on EPB. These findings confirm that marine photochemistry facilitates the nitration of EPB through RNS-mediated processes, generating a stable and potentially more hazardous nitro-product that does not occur in ultrapure waters.

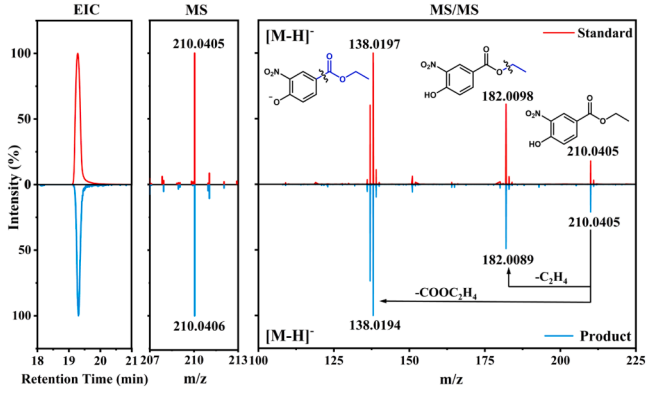

Fig. 3. Extracted ion chromatograms (EIC), Mass Spectrum (MS), and Tandem Mass Spectrum (MS/MS) of nitrated product (NO_2-EPB) and its corresponding standard.

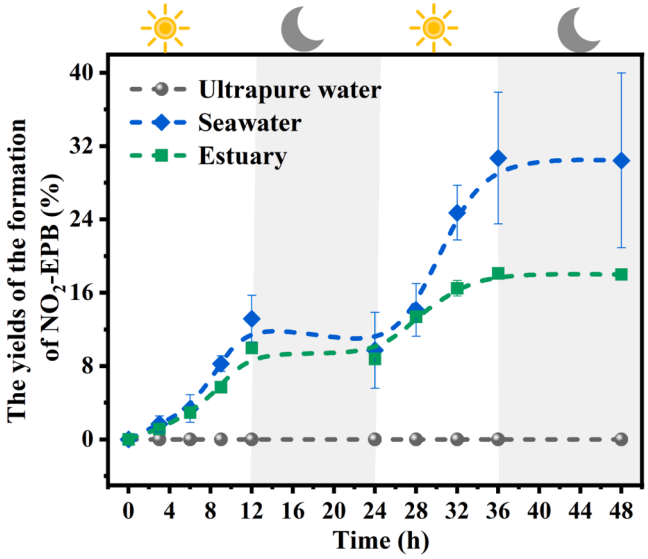

Fig. 4. The yields of NO_2-EPB formed under simulated diurnal solar irradiation in marine, estuarine, and ultrapure water environments.

3.3. Mechanistic insights into coupled nitrogen–pollutant photochemistry

NO_2-EPB forms as a detectable product in marine systems, indicating that nitration is an important transformation pathway of EPB, whereas more photolabile intermediates, such as OH-EPB, rapidly degrade before accumulating to appreciable levels. This transformation is driven by RNS generated through the photolysis of NO_3^- and NO_2^- (Wang et al., 2022; Wu et al., 2020). Under solar irradiation, NO_3^- and NO_2^- absorb ultraviolet light and undergo photochemical reactions, producing radicals such as •OH and •NO_2. While •OH contributes to nonspecific oxidation, •NO_2 acts as an electrophilic nitrating agent with high selectivity toward aromatic compounds containing electron-donating groups, such as phenolic moieties in EPB (Li et al., 2021; Rayaroth et al., 2022).

In seawater and estuarine systems, where the pH typically ranges from 7.5 to 8.5, EPB (pK_a = 8.31) is present predominantly in its neutral form, with only limited deprotonation occurring under environmental conditions (Fig. S4). Under these conditions, nitration reactions can be initiated by •NO_2, which is mainly derived from the photochemical processes involving NO_3^- and NO_2^-. To elucidate the molecular mechanism, two parallel electrophilic substitution pathways between EPB species and •NO_2 were investigated at the molecular level using quantum chemical calculations, denoted as the EPB pathway (R_A) and the EPB$^-$ pathway (R_B). These two mechanistic pathways were proposed based on previous studies of nitration reactions involving phenolic

species (Bedini et al. 2012). The corresponding free energy surfaces of R_A and R_B are illustrated in Fig. 5.

In the R_A pathway, the neutral EPB undergoes a stepwise N-attack addition–elimination mechanism. The addition step proceeds through a transition state (TS_A), in which the nitrogen atom of $\bullet NO_2$ binds to the ortho-carbon adjacent to the hydroxyl group in EPB, with an energy barrier of 28.1 kcal·mol^{-1}, forming the nitrated intermediate (IM_A). Subsequently, IM_A reacts with another $\bullet NO_2$, eliminating a hydrogen atom and yielding nitration products NO_2-EPB via an exothermic process (–14.8 kcal·mol^{-1}). In comparison, the R_B pathway initiates with hydrogen abstraction by $\bullet NO_2$, with a lower transition-state barrier of 19.5 kcal·mol^{-1} to form intermediate IM_{B1}, Subsequently, the addition of another $\bullet NO_2$ to the generated intermediate IM_{B2} produces NO_2-EPB in an exothermic step (–20.7 kcal·mol^{-1}). Notably, the initial addition steps via TS_A and TS_B to form IM_A and IM_B are endothermic; however, solar irradiation can supply sufficient energy to overcome these barriers, facilitating the subsequent exothermic transformations that yield NO_2-EPB as the thermodynamically stable nitration product. Both routes produce thermodynamically stable NO_2-EPB products, in agreement with experimental observations.

These results demonstrate that the photochemical coupling between marine nitrogen species and pollutants reshapes the transformation pathways of emerging contaminants. The generation of $\bullet NO_2$ under environmentally relevant conditions establishes a self-sustaining mechanism in which inorganic nitrogen cycling directly drives organic nitration reactions. This coupling mechanism explains why nitrated products are readily formed in marine matrices but are absent in ultrapure water systems lacking nitrogen donors. The findings highlight the ocean's unique role as both a sink and a reactive medium for anthropogenic pollutants, where nitrogen cycling and photochemistry interact to form more persistent and potentially toxic transformation products.

3.4. Ecotoxicological implications of marine nitration products

The formation of NO_2-EPB in marine environments, a nitrated transformation product showing relative persistence under the tested conditions, raises important ecological and toxicological concerns. Marine-mediated nitration markedly enhances the estrogenic activity of EPB, increasing its potential to act as an endocrine disruptor. In the ERα binding system, the predicted IC_{50} of NO_2-EPB was 59.54 μM, substantially lower than that of the parent compound EPB (76.51 μM),

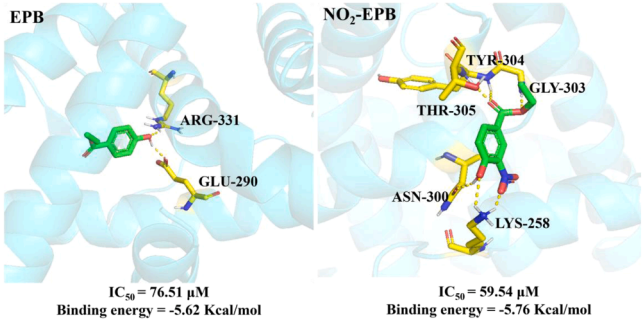

Fig. 6. The binding interaction modes of EPB and its nitration product NO_2-EPB with the estrogen receptor α (ERα) of the Pacific oyster.

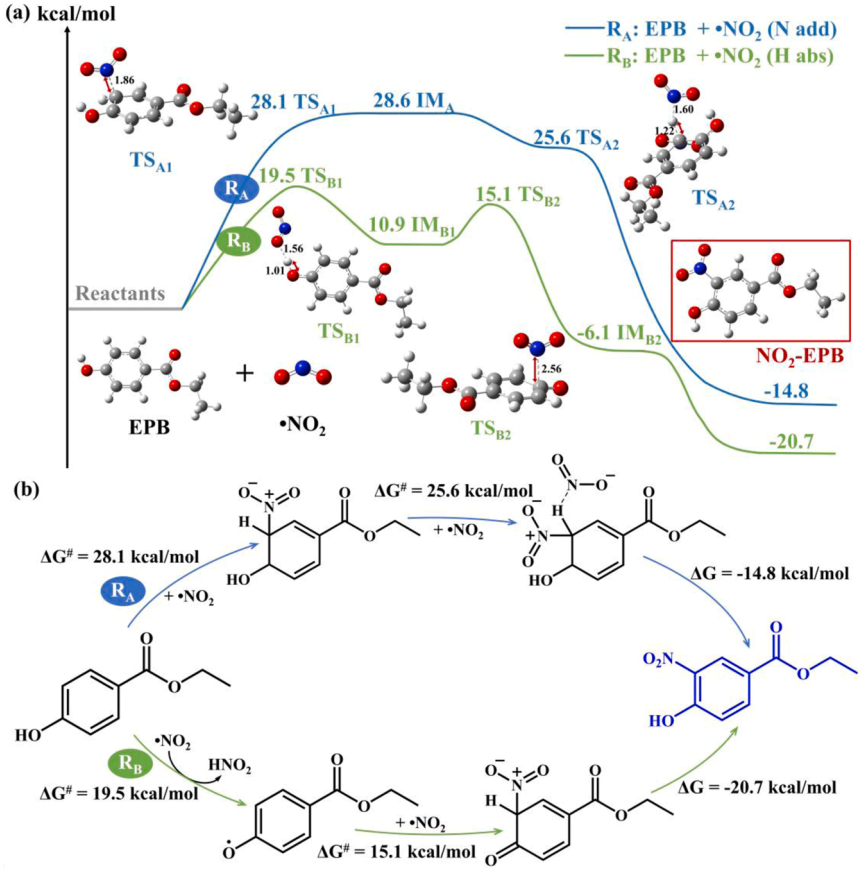

Fig. 5. (a) Free energy surface for the nitration of EPB in seawater (energy in kcal mol^{-1}, bond length in Å): the R_A pathway for neutral EPB (blue) and the R_B pathway for anionic EPB^- (green). (b) Key steps include N-attack via TS_A/TS_B forming intermediates IM_A/IM_B, followed by exothermic formation of NO_2-EPB. Both pathways lead to thermodynamically stable NO_2-EPB, consistent with experimental observations.

indicating that nitration increases receptor-mediated estrogenic effects (Fig. 6). Consistently, NO_2-EPB displayed a lower docking score (–5.76 kcal mol^{-1}) than EPB (–5.62 kcal mol^{-1}). Structural analysis further demonstrated that NO_2-EPB forms hydrogen bonds and hydrophobic interactions with a greater number of amino acid residues in the receptor binding pocket (Fig. 6), suggesting improved binding stability and enhanced endocrine-disrupting potential conferred by nitration. These findings collectively highlight that photochemical nitration in seawater not only transforms the chemical structure of EPB but also generates more potent endocrine-disrupting products, emphasizing the environmental significance posed by persistent nitrated contaminants in marine systems.

From an environmental perspective, NO_2-EPB exhibited minimal degradation during the 12 h dark incubation (<3.5 %), implying relative stability during nighttime or in aphotic seawater layers. To further evaluate the environmental risk, the bioaccumulation and sorption potential of NO_2-EPB were evaluated. NO_2-EPB has a BCF of 37 L/kg and a Koc of 251 L/kg, both slightly higher than EPB (BCF 20 L/kg, Koc 162 L/kg), suggesting a modest increase in accumulation potential in aquatic organisms and sediments. Owing to its hydrophobic and nitroaromatic nature, NO_2-EPB may sorb to particulate matter, potentially reducing freely dissolved concentrations and bioavailability. Consistent with the general resistance of nitroaromatic compounds to aerobic biodegradation, microbial transformation of NO_2-EPB under oxic conditions is expected to be limited, whereas reductive microbial pathways in anoxic or sub-oxic environments may convert nitro groups to nitroso, hydroxylamine, or amine derivatives. Together with its resistance to photodegradation, these characteristics suggest that NO_2-EPB may persist in coastal waters while undergoing slow, environment-dependent transformations. In addition, Danish (Q)SAR predictions indicate that NO_2-EPB exhibits higher mutagenicity and potential carcinogenicity compared to EPB (Table S3), consistent with previous observations that nitrated aromatic compounds often display altered toxicological profiles compared to their parent structures (Rayaroth et al., 2022; Scholes et al., 2019). Taken together with its slightly higher BCF/Koc values, these findings suggest that NO_2-EPB may accumulate in marine organisms, with mutagenic and carcinogenic effects potentially amplified along the food chain, potentially impacting top predators and humans consuming seafood.

Collectively, these findings emphasize that marine photochemical environments—particularly those enriched in reactive nitrogen species—can transform moderately toxic pollutants into more persistent and hazardous products. This underscores the need for long-term environmental monitoring of nitrated transformation products and evaluation of their ecological implications in coastal ecosystems.

4. Conclusion

This study demonstrates that marine environments strongly promote the photochemical degradation and nitration of EPB. The transformation pathway in seawater differs fundamentally from that in ultrapure water, where hydroxylation dominates. Here, nitrate and nitrite photolysis generate reactive nitrogen species that drive electrophilic substitution to form NO_2-EPB. The nitration product exhibits higher persistence and stronger estrogenic activity than its parent compound, indicating elevated ecological risks. Given that all parabens contain a phenolic ring, which can serve as a reactive site for photonitration, the observed photochemical nitration mechanism may be extrapolated to other parabens. Future work should focus on monitoring the occurrence of nitrated parabens in marine waters and effluent-receiving coastal environments to better understand their environmental fate and potential risks. These findings reveal that coupled nitrogen–pollutant photochemistry can convert moderately toxic contaminants into more hazardous products, underscoring the overlooked role of marine nitrogen cycling in shaping the environmental fate and risk of emerging pollutants.

CRediT authorship contribution statement

Yanpeng Gao: Writing – original draft, Visualization, Validation, Supervision, Software, Resources, Project administration, Methodology, Investigation, Funding acquisition, Formal analysis, Data curation. **Yi Chen:** Writing – original draft, Visualization, Validation, Software, Methodology, Investigation, Formal analysis, Data curation. **Suling Wei:** Methodology, Investigation, Data curation. **Yashi Bi:** Methodology, Investigation. **Yujie Chen:** Methodology, Investigation. **Guanhui Chen:** Resources, Methodology, Investigation. **Xiaolin Niu:** Methodology, Investigation. **Na Luo:** Validation, Data curation. **Yuemeng Ji:** Validation, Data curation. **Yang-Guang Gu:** Writing – review & editing, Writing – original draft, Supervision, Data curation, Conceptualization.

Declaration of competing interest

The authors declare that they have no known competing financial interests or personal relationships that could have appeared to influence the work reported in this paper.

Acknowledgments

The authors appreciate the financial supports from the National Key R&D Program of China (2022YFC3105600), National Natural Science Foundation of China (42322704, 42277222), and the Guangdong Basic and Applied Basic Research Foundation (2023B1515020078).

Supplementary materials

Supplementary material associated with this article can be found, in the online version, at doi:10.1016/j.watres.2025.125127.

Data availability

Data will be made available on request.

References

Baker, A.R., Kanakidou, M., Nenes, A., Myriokefalitakis, S., Croot, P.L., Duce, R.A., Gao, Y., Guieu, C., Ito, A., Jickells, T.D., Mahowald, N.M., Middag, R., Perron, M.M.G., Sarin, M.M., Shelley, R. and Turner, D.R. 2021. Changing atmospheric acidity as a modulator of nutrient deposition and ocean biogeochemistry. 7(28), eabd8800.

Bedini, A., Maurino, V., Minero, C., Vione, D., 2012. Theoretical and experimental evidence of the photonitration pathway of phenol and 4-chlorophenol: a mechanistic study of environmental significance. Photochem. Photobiol. Sci. 11 (2), 418–424.

Benedict, K.B., McFall, A.S., Anastasio, C., 2017. Quantum yield of nitrite from the photolysis of aqueous nitrate above 300 nm. Env. Sci. Techn. 51 (8), 4387–4395.

Bolujoko, N.B., Ogunlaja, O.O., Alfred, M.O., Okewole, D.M., Ogunlaja, A., Olukanni, O. D., Msagati, T.A.M., Unuabonah, E.I., 2022. Occurrence and human exposure assessment of parabens in water sources in Osun State, Nigeria. Sci. Total. Environ. 814, 152448.

Bu, L., Zhu, N., Li, C., Huang, Y., Kong, M., Duan, X., Dionysiou, D.D., 2020. Susceptibility of atrazine photo-degradation in the presence of nitrate: impact of wavelengths and significant role of reactive nitrogen species. J. Hazard. Mater. 388, 121760.

Calza, P., Vione, D., Novelli, A., Pelizzetti, E., Minero, C., 2012. The role of nitrite and nitrate ions as photosensitizers in the phototransformation of phenolic compounds in seawater. Sci. Total. Environ. 439, 67–75.

Chen, G., Hanukovich, S., Chebeir, M., Christopher, P., Liu, H., 2019. Nitrate removal via a formate radical-induced photochemical process. Env. Sci. Techn. 53 (1), 316–324.

Du, L., Guo, W., Li, D., Tillotson, M.R., Zhu, Y., Yue, J., Li, J., Huo, S., Gao, Y., Zhao, X., 2025. Invisible threats from typical endocrine disrupting compounds in estuarine environments caused by continuing seawater incursion: in-situ evidence of biogeochemical processes captured by diffusive gradients in thin films. Water. Res. 281, 123605.

Fang, H.S., Gao, Y.P., Li, G.Y., An, J.B., Wong, P.K., Fu, H.Y., Yao, S.D., Nie, X.P., An, T. C., 2013. Advanced oxidation kinetics and mechanism of preservative propylparaben degradation in aqueous suspension of TiO2 and risk assessment of its degradation products. Env. Sci. Techn. 47 (6), 2704–2712.

Frisch, M.J., Trucks, G.W., Schlegel, H.B., Scuseria, G.E., Robb, M.A., Cheeseman, J.R., Scalmani, G., Barone, V., Petersson, G.A., Nakatsuji, H., Li, X., Caricato, M., Marenich, A.V., Bloino, J., Janesko, B.G., Gomperts, R., Mennucci, B., Hratchian, H. P., Ortiz, J.V., Izmaylov, A.F., Sonnenberg, J.L., Williams, D.F., Lipparini, F., Egidi, F., Goings, J., Peng, B., Petrone, A., Henderson, T., Ranasinghe, D., Zakrzewski, V.G.,

Gao, J., Rega, N., Zheng, G., Liang, W., Hada, M., Ehara, M., Toyota, K., Fukuda, R., Hasegawa, J., Ishida, M., Nakajima, T., Honda, Y., Kitao, O., Nakai, H., Vreven, T., Throssell, K., Montgomery Jr., J.A., Peralta, J.E., Ogliaro, F., Bearpark, M.J., Heyd, J. J., Brothers, E.N., Kudin, K.N., Staroverov, V.N., Keith, T.A., Kobayashi, R., Normand, J., Raghavachari, K., Rendell, A.P., Burant, J.C., Iyengar, S.S., Tomasi, J., Cossi, M., Millam, J.M., Klene, M., Adamo, C., Cammi, R., Ochterski, J.W., Martin, R. L., Morokuma, K., Farkas, O., Foresman, J.B. and Fox, D.J. 2009. Gaussian 09 Rev. D.01. Wallingford, CT.

Gao, Y.P., Ji, Y.M., Li, G.Y., An, T.C., 2014. Mechanism, kinetics and toxicity assessment of OH-initiated transformation of triclosan in aquatic environments. Water. Res. 49, 360–370.

Gao, Y., Niu, X., Qin, Y., Guo, T., Ji, Y., Li, G., An, T., 2020. Unexpected culprit of increased estrogenic effects: oligomers in the photodegradation of preservative ethylparaben in water. Water. Res. 176, 115745.

Ge, L.K., Na, G.S., Chen, C.E., Li, J., Ju, M.W., Wang, Y., Li, K., Zhang, P., Yao, Z.W., 2016. Aqueous photochemical degradation of hydroxylated PAHs: kinetics, pathways, and multivariate effects of main water constituents. Sci. Total. Environ. 547, 166–172.

Ge, J., Huang, D., Han, Z., Wang, X., Wang, X., Wang, Z., 2019. Photochemical behavior of benzophenone sunscreens induced by nitrate in aquatic environments. Water. Res. 153, 178–186.

Godfrey, L.V., Omta, A.W., Tziperman, E., Li, X., Hu, Y., Falkowski, P.G., 2025. Stability of the marine nitrogen cycle over the past 165 million years. Nat. Commun. 16 (1), 8982.

Gong, S., Ding, C., Liu, J., Fu, K., Pan, Y., Shi, J., Deng, H., 2022. Degradation of Naproxen by UV-irradiation in the presence of nitrate: efficiency, mechanism, products, and toxicity change. Chem. Eng. J. 430, 133016.

Gong, C., Tian, H., Liao, H., Pan, N., Pan, S., Ito, A., Jain, A.K., Kou-Giesbrecht, S., Joos, F., Sun, Q., Shi, H., Vuichard, N., Zhu, Q., Peng, C., Maggi, F., Tang, F.H.M., Zaehle, S., 2024. Global net climate effects of anthropogenic reactive nitrogen. Nature 632 (8025), 557–563.

Li, Y., Qin, H., Li, Y., Lu, J., Zhou, L., Chovelon, J.M., Ji, Y., 2021. Trace level nitrite sensitized photolysis of the antimicrobial agents parachlormetaxylenol and chlorophene in water. Water. Res. 200, 117275.

Liu, G., Shen, L., Ciais, P., Lin, X., Hauglustaine, D., Lan, X., Turner, A.J., Xi, Y., Zhu, Y., Peng, S., 2025. Trends in the seasonal amplitude of atmospheric methane. Nature 641 (8063), 660–665.

Lu, S., Wang, J., Wang, B.D., Xin, M., Lin, C.Y., Gu, X., Lian, M.S., Li, Y., 2023. Comprehensive profiling of the distribution, risks and priority of pharmaceuticals and personal care products: a large-scale study from rivers to coastal seas. Water. Res. 230.

Marenich, A.V., Cramer, C.J., Truhlar, D.G., 2009. Universal solvation model based on solute electron density and on a continuum model of the solvent defined by the bulk dielectric constant and atomic surface tensions. J. Phys. Chem. B 113 (18), 6378–6396.

Marussi, G., Vione, D., 2021. Secondary formation of aromatic nitroderivatives of environmental concern: photonitration processes triggered by the photolysis of nitrate and nitrite ions in aqueous solution. Molecules 26 (9), 2550.

McDowell, R.W., Luo, D., Pletnyakov, P., Upsdell, M., Dodds, W.K., 2025. Anthropogenic nutrient inputs cause excessive algal growth for nearly half the world's population. Nat. Commun. 16 (1), 1830.

MEFD (Ministry of Environment and Food of Denmark), 2025. Danish (Q)SAR models of webpage or database. Available at: https://qsarmodels.food.dtu.dk/index.html.

Niu, X., Chen, G., Luo, N., Wang, M., Ma, M., Hui, X., Gao, Y., Li, G., An, T., 2025. The association between estrogenic activity evolution and the formation of different products during the photochemical transformation of parabens in water. Water. Res. 276, 123236.

Palma, D., Arbid, Y., Sleiman, M., de Sainte-Claire, P., Richard, C., 2020. New route to toxic nitro and nitroso products upon irradiation of micropollutant mixtures containing imidacloprid: role of NO_x and effect of natural organic matter. Env. Sci. Technol. 54 (6), 3325–3333.

Peng, A., Wang, C., Zhang, Z., Jin, X., Gu, C., Chen, Z., 2022. Tetracycline photolysis revisited: overlooked day-night succession of the parent compound and metabolites in natural surface waters and associated ecotoxicity. Water. Res. 225, 119197.

Peng, F.J., Zhu, R.G., Pan, C.G., Zhou, C.Y., Hu, J.J., Li, S., Feng, X.J., Yu, K.F., 2025. Parabens and their metabolites in surface sediment from estuaries to the sea: occurrence, spatial distribution, and potential sources. ACS. ES. T. Water. 5 (7), 3739–3748.

Rayaroth, M.P., Aravindakumar, C.T., Shah, N.S., Boczkaj, G., 2022. Advanced oxidation processes (AOPs) based wastewater treatment - unexpected nitration side reactions - a serious environmental issue: a review. Chem. Eng. J. 430, 133002.

Scholes, R.C., Prasse, C., Sedlak, D.L., 2019. The role of reactive nitrogen species in sensitized photolysis of wastewater-derived trace organic contaminants. Env. Sci. Technol. 53 (11), 6483–6491.

Scholes, R.C., 2022. Emerging investigator series: contributions of reactive nitrogen species to transformations of organic compounds in water: a critical review. Environ. Sci.. 24 (6), 851–869.

Schwarzenbach, R.P., Escher, B.I., Fenner, K., Hofstetter, T.B., Johnson, C.A., von Gunten, U., Wehrli, B., 2006. Chall. Micropollutants Aquat. Syst. 313 (5790), 1072–1077.

Schymanski, E.L., Jeon, J., Gulde, R., Fenner, K., Ruff, M., Singer, H.P., Hollender, J., 2014. Identifying small molecules via high resolution mass spectrometry: communicating confidence. Env. Sci. Technol. 48 (4), 2097–2098.

Tait, D.R., Santos, I.R., Lamontagne, S., Sippo, J.Z., McMahon, A., Jeffrey, L.C., Maher, D. T., 2023. Submarine groundwater discharge exceeds river inputs as a source of nutrients to the great barrier reef. Env. Sci. Technol. 57 (41), 15627–15634.

Troughton, J., Gasparini, N., Baran, D., 2018. $Cs_{0.15}FA_{0.85}PbI_3$ perovskite solar cells for concentrator photovoltaic applications. J. Mater. Chem. A 6 (44), 21913–21917.

USEPA, 2012. Estimation programs interface suite™ for Microsoft® Windows of webpage or database. Available at: https://www.epa.gov/tsca-screening-tools/epi-suitetm-estimation-program-interface.

Vione, D., Maurino, V., Minero, C., Pelizzetti, E., 2002. New processes in the environmental chemistry of nitrite: nitration of phenol upon nitrite photoinduced oxidation. Env. Sci. Technol. 36 (4), 669–676.

Vione, D., Maurino, V., Minero, C., Pelizzetti, E., 2005. Reactions induced in natural waters by irradiation of nitrate and nitrite ions. Hdb. Env. Chem. 2, 221–253.

Vione, D., 2022. A model assessment of the occurrence and reactivity of the nitrating/nitrosating agent nitrogen dioxide ($\bullet NO_2$) in sunlit natural waters. Molecules 27 (15), 4855.

Wang, J., Wang, K., Guo, Y., Niu, J., 2020. Photochemical degradation of nebivolol in different natural organic matter solutions under simulated sunlight irradiation: kinetics, mechanism and degradation pathway. Water. Res. 173, 115524.

Wang, Y., Yin, R., Tang, Z., Liu, W., He, C., Xia, D., 2022. Reactive nitrogen species mediated inactivation of pathogenic microorganisms during UVA photolysis of nitrite at surface water levels. Env. Sci. Technol. 56 (17), 12542–12552.

Wang, X., Wang, W., Wingen, L.M., Perraud, V., Ezell, M.J., Gable, J., Poulos, T.L. and Finlayson-Pitts, B.J. 2023. Predicting the environmental fates of emerging contaminants: synergistic effects in ozone reactions of nitrogen-containing alkenes. 9 (9), eade9609.

Wang, M., Bodirsky, B.L., Rijneveld, R., Beier, F., Bak, M.P., Batool, M., Droppers, B., Popp, A., van Vliet, M.T.H., Strokal, M., 2024. A triple increase in global river basins with water scarcity due to future pollution. Nat. Commun. 15 (1), 880.

Wei, F., Mortimer, M., Cheng, H., Sang, N., Guo, L.H., 2021. Parabens as chemicals of emerging concern in the environment and humans: a review. Sci. Total. Environ. 778, 146150.

Wilkinson, J.L., Boxall, A.B.A., Kolpin, D.W., Leung, K.M.Y., Lai, R.W.S., Galbán-Malagón, C., Adell, A.D., Mondon, J., Metian, M., Marchant, R.A., Bouzas-Monroy, A., Cuni-Sanchez, A., Coors, A., Carriquiriborde, P., Rojo, M., Gordon, C., Cara, M., Moermond, M., Luarte, T., Petrosyan, V., Perikhanyan, Y., Mahon, C.S., McGurk, C. J., Hofmann, T., Kormoker, T., Iniguez, V., Guzman-Otazo, J., Tavares, J.L., Gildasio De Figueiredo, F., Razzolini, M.T.P., Dougnon, V., Gbaguidi, G., Traoré, O., Blais, J. M., Kimpe, L.E., Wong, M., Wong, D., Ntchantcho, R., Pizarro, J., Ying, G.G., Chen, C.E., Páez, M., Martínez-Lara, J., Otamonga, J.P., Poté, J., Ifo, S.A., Wilson, P., Echeverría-Sáenz, S., Udikovic-Kolic, N., Milakovic, M., Fatta-Kassinos, D., Ioannou-Ttofa, L., Belušová, V., Vymazal, J., Cárdenas-Bustamante, M., Kassa, B.A., Garric, J., Chaumot, A., Gibba, P., Kunchulia, I., Seidensticker, S., Lyberatos, G., Halldórsson, H.P., Melling, M., Shashidhar, T., Lamba, M., Nastiti, A., Supriatin, A., Pourang, N., Abedini, A., Abdullah, O., Gharbia, S.S., Pilla, F., Chefetz, B., Topaz, T., Yao, K.M., Aubakirova, B., Beisenova, R., Olaka, L., Mulu, J.K., Chatanga, P., Ntuli, V., Blama, N.T., Sherif, S., Aris, A.Z., Looi, L.J., Niang, M., Traore, S.T., Oldenkamp, R., Ogunbanwo, O., Ashfaq, M., Iqbal, M., Abdeen, Z., O'Dea, A., Morales-Saldaña, J.M., Custodio, M., de la Cruz, H., Navarrete, I., Carvalho, F., Gogra, A.B., Koroma, B.M., Cerkvenik-Flajs, V., Gombač, M., Thwala, M., Choi, K., Kang, H., Ladu, J.L.C., Rico, A., Amerasinghe, P., Sobek, A., Horlitz, G., Zenker, A.K., King, A.C., Jiang, J.J., Kariuki, R., Tumbo, M., Tezel, U., Onay, T.T., Lejju, J.B., Vystavna, Y., Vergeles, Y., Heinzen, H., Pérez-Parada, A., Sims, D.B., Figy, M., Good, D. and Teta, C. 2022. Pharmaceutical pollution of the world's rivers. 119(8), e2113947119.

Wu, Y., Bu, L., Duan, X., Zhu, S., Kong, M., Zhu, N., Zhou, S., 2020. Mini review on the roles of nitrate/nitrite in advanced oxidation processes: radicals transformation and products formation. J. Clean. Prod. 273, 123065.

Xue, X., Xue, J., Liu, W., Adams, D.H., Kannan, K., 2017. Trophic magnification of parabens and their metabolites in a subtropical marine food web. Env. Sci. Technol. 51 (2), 780–789.

Yin, R., Dao, P.U., Zhao, J., Wang, K., Lu, S.H., Shang, C., Ren, H.Q., 2024. Reactive nitrogen species generated from far-UVC photolysis of nitrate contribute to pesticide degradation and nitrogenous byproduct formation. Env. Sci. Technol. 58 (46), 20676–20686.

Zhang, T., Dong, J., Ji, Y., Kong, D., Lu, J., 2022. Photodegradation of benzophenones sensitized by nitrite. Sci. Total. Environ. 802, 149850.

Zhao, Y., Truhlar, D.G., 2008. The M06 suite of density functionals for main group thermochemistry, thermochemical kinetics, noncovalent interactions, excited states, and transition elements: two new functionals and systematic testing of four M06-class functionals and 12 other functionals. Theor. Chem. Acc. 120 (1), 215–241.

Zhou, S., Li, L., Wu, Y., Zhu, S., Zhu, N., Bu, L., Dionysiou, D.D., 2020. UV365 induced elimination of contaminants of emerging concern in the presence of residual nitrite: roles of reactive nitrogen species. Water. Res. 178, 115829.

Zhu, R.G., Pan, C.G., Peng, F.J., Zhou, C.Y., Hu, J.J., Yu, K.F., 2024. Parabens and their metabolite in a marine benthic-dominated food web from the Beibu gulf, South China Sea: occurrence, trophic transfer and health risk assessment. Water. Res. 248.